Preparation of a novel flame retardant based on phosphorus/nitrogen modified lignin with metal–organic framework and its application in epoxy resin
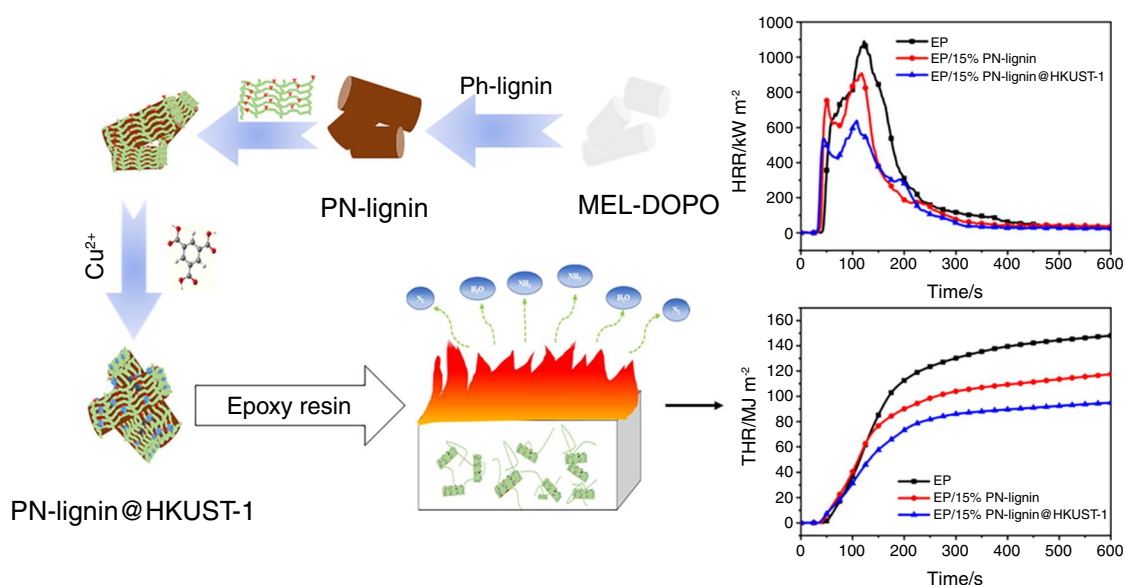
Hongyu Yang[1] · Yu Qin[1] · Dingxiang Liang[1] · Xinyu Lu[1] · Xiaoli Gu[1]

Abstract

To reduce the fire risk of epoxy (EP) resin, a renewable lignin-based flame retardant functionalized with a metal–organic framework (MOF) HKUST-1 ($Cu_3(BTC)_2$, BTC = benzene-1,3,5-tricarboxylate) was prepared by a facile and green method. The chemical structure of flame retardant was characterized by Fourier transform infrared (FTIR) spectroscopy, X-ray photoelectron spectroscopy (XPS), X-ray diffraction (XRD) and scanning electron microscopy (SEM). The results showed that HKUST-1 was *in-situ* grown on the surface of phosphorus/nitrogen modified lignin, which was treated as an efficient flame retardant (termed PN-lignin@HKUST-1) for subsequent EP resin. The flame-retardant properties of EP composites were evaluated by the limiting oxygen index (LOI), vertical burning (UL-94), and cone calorimetry tests. As compared with neat EP thermoset, the presence of 15 mass% PN-lignin@HKUST-1 increased the LOI value from 28.5 to 33.2% and upgraded the UL-94 rating from V-2 to V-0. Besides, the peak heat release rate (PHRR) and total heat release (THR) were reduced by 41.2 and 33.8%, respectively. Observations of char residues could indicate that addition of PN-lignin@HKUST-1 contributes to a compact and dense char layer, which blocks the release and transfer of heat and harmful gases during combustion.

Graphic abstract

Keywords HKUST-1 · Lignin · Flame retardant · Epoxy resin

Introduction

As a conventional thermosetting plastic, epoxy (EP) resin is widely used in daily life, such as automotive adhesives, building decoration, electronic device insulating material [1–4]. Epoxy resins can be divided into five categories according to molecular structure, i.e., bisphenol-A epoxy resins, bisphenol-F epoxy resins, aliphatic glycidyl ether epoxy resin, glycidyl ester type epoxy resin and polyphenol type glycidyl ether epoxy resin. Among them, the most considerable output is bisphenol-A epoxy resin, which accounts for 90% of the epoxy resin applied in the world [5]. Due to its excellent adhesion, high strength, electrical insulation and corrosion resistance, epoxy resin plays an increasingly significant role in many industries including laminates, adhesives, electronic/electrical industries [6, 7]. However, the limiting oxygen index (LOI) of epoxy resin is only about 26%, which means it is very flammable in air and seriously limits its application in many cases [8]. Therefore, it is of great necessity and importance to develop a more efficient system to further improve the flame-retardant properties of epoxy resin.

The most common and effective method was adding flame retardants in the preparation of epoxy resin. Traditional flame retardants were usually halogen-flame retardants. Despite its outstanding fire resistance, epoxy resins containing halogen element flame retardants would produce toxic fumes during combustion, which were harmful to the environment and human health [9]. Hence, there was a desire need to explore eco-friendly flame retardants to replace halogen-flame retardants. Compared with traditional flame retardants, intumescent flame retardants had the characteristics of high carbon content, good flame-retardant effect and environmental protection. Intumescent flame retardants were constituted of the acid, carbon and gas sources, which expanded rapidly to form protective char layers. The carbon source was mainly polyhydroxy compounds, such as pentaerythritol and ethylene glycol. With the continuous research on biomass resources in recent years, it had been discovered that lignin can also be used as a carbon source [10].
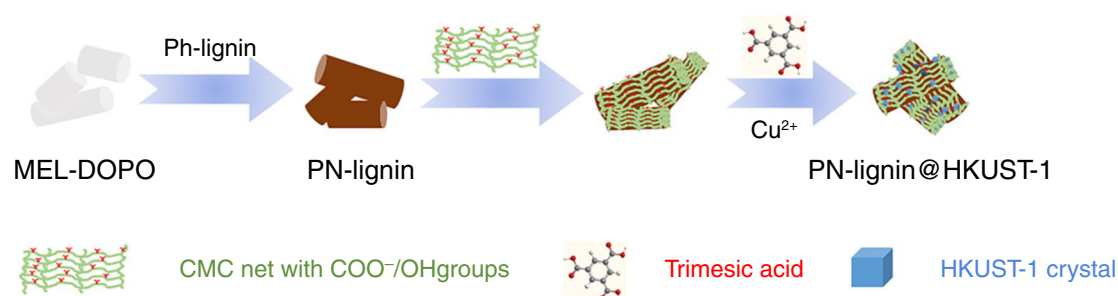
Lignin is one of the essential components of plant cell wall and is also the second most abundant renewable resource in nature next to cellulose [11–13]. It is a biopolymer containing many aromatic ring structures and different functional groups, namely carbonyl, carboxyl, methoxyl, aliphatic and aromatic hydroxyl moieties [14]. On account of the high carbon yield after decomposition, lignin has received extensive attention in the preparation of bio-based flame retardants. It was reported that about 35–40% of carbon can be produced after pyrolysis of lignin [15]. At that point, lignin can be incorporated into

polymers to improve the thermodynamic properties of the material. Besides, chemical modification of lignin and the introduction of flame-retardant elements such as phosphorus and nitrogen could enhance the flame-retardant performance of lignin-based composites [16–20].

In the past several years, 9,10-dihydro-9-oxa-10-phosphaphenanthrene-10-oxide (DOPO) had been reported as an inorganic phosphorus flame-retardant intermediate since it could serve as an acid and gas source [21, 22]. Its molecular structure contained a P–H bond, biphenyl ring and phenanthrene ring, with a higher thermal and chemical stability than the general, noncyclic organophosphate [23–27]. Due to these unique advantages, lignin-based flame retardants modified with DOPO could significantly improve flame-retardant effect, which showed great potential and broad application prospects [28].

Currently, metal–organic frameworks (MOFs) have attracted widespread interest for their superior capabilities and unique properties on the fields of fire-proof and flame retarding [29–31]. In a word, MOFs are crystalline porous materials with a periodic network structure, consisting of inorganic metal centers (metal ions or metal clusters) and bridging organic ligands connected by self-assembly [32]. The organic groups on the branches can also contain phosphorus, nitrogen and other flame-retardant elements [33]. In addition, by reason of large pore volume and specific surface area, MOFs can absorb toxic gas and improve the smoke-suppression performance of polymer materials [34]. Furthermore, MOFs have many unsaturated metal sites that can provide active catalytic centers for catalytic oxidation of CO, which can reduce the amount of CO released during combustion [35]. Hence, the introduction of MOFs structure to epoxy resin is a promising attempt to achieve the solution.

In this work, research was aimed at promoting the high value-added utilization of industrial lignin and improving the flame resistance of epoxy (EP) resin. The phenolated alkali lignin was functionalized by coordinating the grafting of nitrogen and phosphorus (melamine and DOPO mixture) (referred to as PN-lignin) and further cellulose foam HKUST-1 ($Cu_3(BTC)_2$, BTC = benzene-1,3,5-tricarboxylate) structure, which is one of the MOFs, was introduced by a green and convenient method (as shown in Scheme 1). The chemical composition and structure of prepared flame retardant (referred to as PN-lignin@HKUST-1) were characterized by Fourier transform infrared (FTIR), X-ray diffraction (XRD) and X-ray photoelectron spectra (XPS). Epoxy resin was subsequently cured to fabricate EP composites by blending with as-prepared flame retardant (referred to as EP/PN-lignin@HKUST-1). The surface morphologies of PN-lignin@HKUST-1 and EP/PN-lignin@HKUST-1 were observed by scanning electron microscopy (SEM), and thermal behaviors were determined by thermogravimetric analysis (TGA). The flame-retardant properties of EP/

Scheme 1 Synthesis of PN-lignin@HKUST-1 as EP flame-retardant additive

PN-lignin@HKUST-1 composites were also measured by limiting oxygen index (LOI), vertical burning (UL-94), and cone calorimetry tests. This article would provide valuable information for the flame-retardant modification of lignin and reliable reference for the application of HKUST-1 based on lignin in epoxy resin.

Experimental

Materials

Alkaline lignin (Al-lignin) was purchased from TCI Shanghai Co. Ltd., China. DOPO, carboxymethyl cellulose sodium (CMC) and 4,4-diaminodiphenylmethane (DDM) were provided by Shanghai Macklin Co. Ltd., China. Diglycidyl ether of bisphenol-A type epoxy resin (commercial name: E 51) was purchased from Xingchen Epoxy Resins Factory (Nantong, China). Melamine (MEL) was obtained from Shanghai Lingfeng Co. Ltd., China. Formaldehyde, N,N-dimethylformamide (DMF), anhydrous copper acetate (Cu(OAc)$_2$), trimesic acid (H$_3$BTC), glacial acetic acid (CH$_3$COOH), diethyl ether, ethanol and phenol were purchased from Nanjing Chemical Reagent Co. Ltd., China.

Phenolation of alkaline lignin (Ph-lignin)

First, 20.00 g of Al-lignin was added to a flask containing 80 mL of H$_2$SO$_4$ solution (2.00 mol L^{-1}), heated up to 80 °C and stirred for 1.5 h. Then, when the temperature was raised to 95 °C, 18.00 g of phenol (0.20 mol L^{-1}) was added, and the mixture was stirred at reflux for 1.5 h. After the reaction was completed, the mixture was washed three times by 500 mL of diethyl ether and dried in a vacuum oven at 70 °C overnight to a constant mass.

Preparation of MEL and DOPO mixture (MEL-DOPO)

12.96 g of DOPO (0.06 mol) was added to 280 mL of ethanol aqueous solution (70 mass%) and stirred for 30 min,

allowing the DOPO to be fully dispersed in the solution. Then, 10.00 g of MEL (0.08 mol) was added and stirred for 6 h when the temperature was raised to 70 °C. After completion, the mixture was cooled to room temperature, washed repeatedly with ethanol three times and dried in the vacuum oven at 70 °C for 12 h.

Preparation of PN-lignin

Approximately 4.00 g of phenolated lignin, 20.00 g of MEL-DOPO (mass ratio, Ph-lignin/MEL-DOPO = 1:5) and 7.20 g (0.24 mol) of formaldehyde were added to a flask with 300 mL of DMF and stirred under reflux condition at 75 °C for 3 h. After the reaction was finished, 500 mL of distilled water was added and the solid was filtered, washed three times with 500 mL of distilled water and dried at 70 °C under vacuum for 24 h.

Preparation of PN-lignin@HKUST-1

First of all, accurately 1.47 g of CMC (6.06 mol) with 2.00 g of PN-lignin was added into 70 mL of deionized water and mechanically stirred under room temperature for 1 h. Secondly, 1.33 g of Cu(OAc)$_2$ (6.64 mmol) dissolved in 30 mL of deionized water and 1 mL of HAc were added dropwise and kept in stirring for 5 min. Thirdly, 1.15 g of H$_3$BTC (5.50 mmol) dissolved in 15 mL ethanol was sequentially added, and the mixture was continuously stirred in a closed system for 4 h. Finally, the end product was obtained by centrifugation and dried in the vacuum oven at 70 °C for 24 h.

Preparation of flame-retardant EP composites

A traditional curing method was applied to fabricate epoxy composites with some modifications. Typically, 3.00 g of PN-lignin@HKUST-1 and 15.00 g of EP were mechanically stirred at 1000 rpm for 1.5 h to obtain a uniform mixture system. Next, 3.00 g of curing agent DDM (mass ratio, DDM/ EP = 1:5) was added and kept in stirring for 1.5 h. The uniformly mixed thermoset was poured into the mold

Table 1 Information about lignin-based materials

Sample	Components
Al-lignin	Alkaline lignin
ph-lignin	Phenolation of Al-lignin
PN-lignin	ph-lignin mixed with MEL-DOPO
EP/PN-lignin	PN-lignin mixed with epoxy resin
PN-lignin@HKUST-1	PN-lignin loaded by HKUST-1
EP/PN-lignin@HKUST-1	EP/PN-lignin loaded by HKUST-1

and cured at 100 °C for 2 h after bubbles were removed in the vacuum oven. For further curing, the temperature was raised to 150 °C for 2 h. To evaluate the effect of modification, the neat EP thermoset and EP composites containing PN-lignin (referred to as EP/PN-lignin) were also prepared according to the similar procedure.

Above, lignin-based materials information was listed in Table 1.

Measurements

The Fourier transform infrared (FTIR) spectra were recorded with a Nicolet 6700 FTIR spectrometer by using compressed potassium bromide (KBr) disks. The scanning range of infrared spectrometer was 4000–500 cm^{-1} with 32 scans per spectrum. The thermogravimetric analysis (TGA) was obtained on DTG-60AH (SHIMADZU, Japan). The epoxy resin composites (about 5 mg) were heated (30–800 °C) at a rate of 20 °C min^{-1} under the nitrogen flow of 20 mL min^{-1}. The X-ray diffraction (XRD) patterns were tested with the Japanese Ultima IV combined multifunctional horizontal X-ray diffraction spectrometer. The scanning speed was 10° min^{-1}, and the scanning diffraction angle 2θ was 5–80°. The X-ray photoelectron spectroscopy (XPS) spectra were recorded by an AXIS UltraDLD spectrometer with Al Kα (1486.6 eV) radiation. The surface morphologies of samples were observed using a JEOLJSM-7600 scanning electron microscopy (SEM) (JEOL, Japan) at the accelerating voltage of 15 kV. The limiting oxygen index (LOI) values of composites were measured using an HC-2C oxygen index meter (Jiangsu Institute of Chemical Industry, China). The size of three samples was 100 mm × 10 mm × 3 mm according to ASTM D2863-97 standard. The Vertical burning (UL-94) test was conducted on a CZF-2 instrument (Jiangsu Institute of Chemical Industry, China), and the size of three epoxy resin composites was 100 mm × 10 mm × 3 mm according to ATSM D3801 standard. The combustion behavior of the samples was measured by a cone calorimeter (Fire Testing Technology, UK). For each formulation, the samples (100 mm × 100 mm × 3.2 mm dimension) were exposed to a radiant cone under a heat flux of 50 kW m^{-2} according to ISO 5660 standard. The samples were backed with
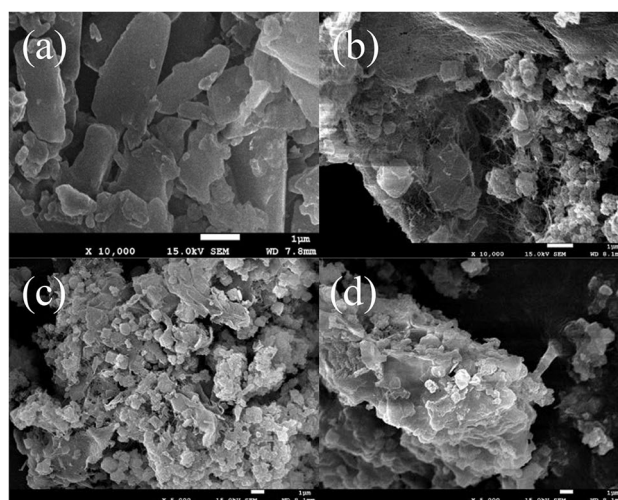
aluminum foil in a metal frame. Laser Raman spectroscopy (LRS) was also used to test the residue by configuring a laser system with a wavelength of 532 nm.
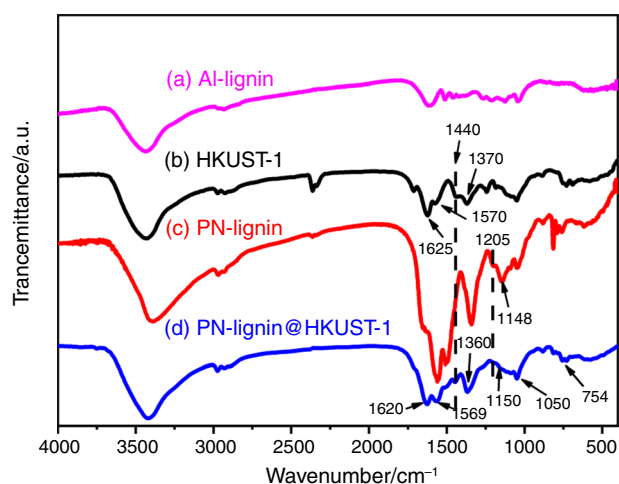
Results and discussion

Characterization of prepared flame retardants

As shown in Fig. 1a, DOPO is predominantly columnar in shape with a varying length and relatively smooth surface. It can be seen from Fig. 1b that foam HKUST-1 displays the shape of cubic crystal, which is consistent with previous report [36]. The crystal surface is also covered with a thin web of fibers since HKUST-1 crystals are grown from the copper irons (Cu^{2+}) bridging of CMC chains and ligands. From Fig. 1c, d, it shows that the surface of DOPO columns becomes coarse and irregular. It is because DOPO is coated with lignin by Mannich reaction between lignin and MEL to form PN-lignin. There are many small cubes unevenly distributed on the surface of PN-lignin@HKUST-1, and the fiber webs are not particularly obvious, which is due to the adhesion of CMC to the surface of lignin and then, the adsorption of metal ions to generate HKUST-1. Furthermore, the size of foam HKUST-1 slightly decreases because the growth of HKUST-1 on the lignin surface is restricted. It may be because Cu^{2+} is adsorbed to the surface under the effect of CMC [37]. These results preliminarily indicate that DOPO is coated with lignin and HKUST-1, and consequently flame retardant PN-lignin@HKUST-1 is prepared.
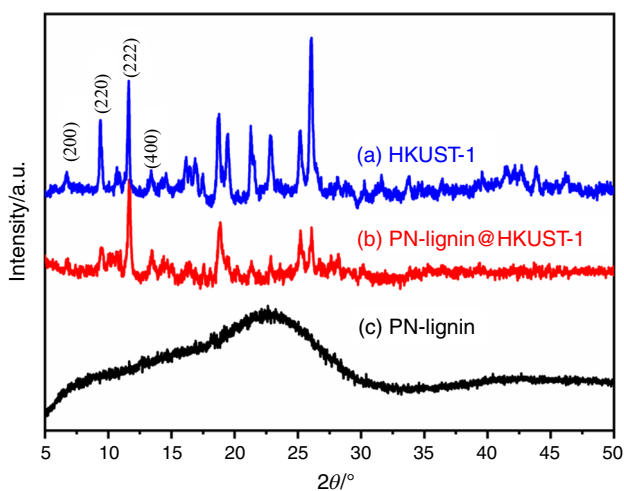
To demonstrate the chemical structure of the as-prepared samples, the FTIR spectra are performed and presented in Fig. 2. The absorption peaks at 1625/1570 and

Fig. 1 SEM images of DOPO (**a**), foam HKUST-1 (**b**) at 10,000 times magnification, and PN-lignin@HKUST-1 (**c**, **d**) at 5000 times magnification

Fig. 2 FTIR spectra of Al-lignin (**a**), HKUST-1 (**b**), PN-lignin (**c**) and PN-lignin@HKUST-1 (**d**)

Fig. 3 XRD spectra of foam HKUST-1 (**a**), PN-lignin@HKUST-1 (**b**) and PN-lignin (**c**)

1440/1370 cm^{-1} are attributed to –COOH and –CH$_2$–/–CH$_3$ in foam HKUST-1, respectively [38]. The absorption peaks of 754, 1205 and 1569 cm^{-1} are assigned to the stretching vibrations of P–O–Ph, P=O and P–Ph, which belong to DOPO structure [39, 40]. Moreover, the presence of P–O–C vibration can be observed at 1050 cm^{-1}. The appearance of these characteristic absorption peaks in the FTIR spectrum of PN-lignin@HKUST-1 confirms that DOPO and HKUST-1 are successfully introduced into modified lignin [41].
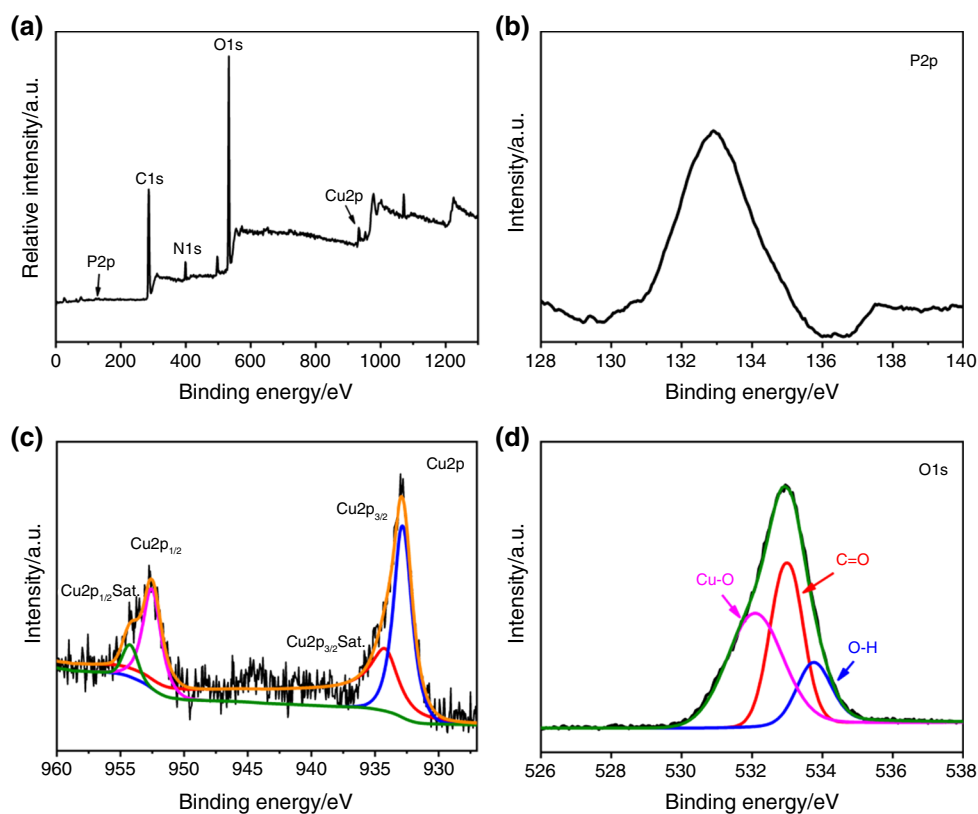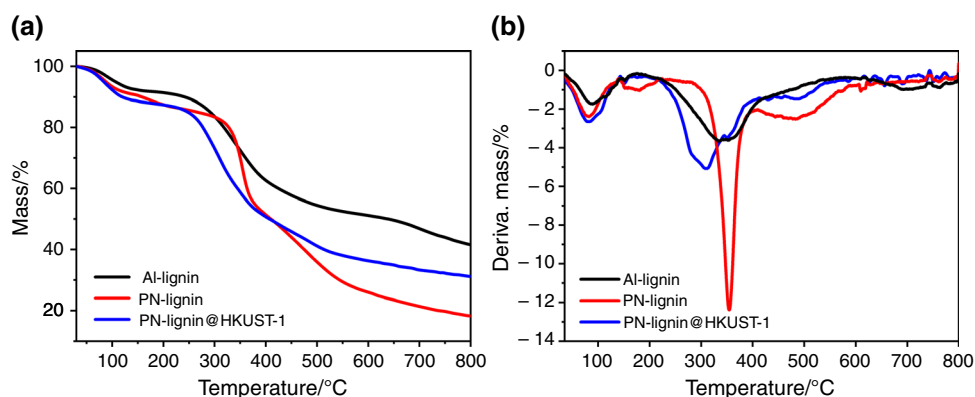
The crystal structures of foam HKUST-1 and synthesized flame retardant are determined by XRD. As shown in Fig. 3a, the XRD spectrum suggests the intact diffraction characteristic peak profiles of HKUST-1 [42]. In peculiar, the appearance of lattice plane in (200) facet is due to the

formation of cubic crystal structure, as evidenced by SEM observations [36]. From Fig. 3b, it reveals that the characteristic peaks of PN-lignin@HKUST-1 are the same as those of HKUST-1 except that their peak intensity is weakened. It is because only part of the crystal structure of HKUST-1 is exposed on the surface, and the rest is covered by functionalized lignin or destroyed after adsorption [43]. Besides, the peak of PN-lignin (Fig. 3c) disappears when HKUST-1 has been loaded, which is mainly because of the high intensity of HKUST-1 characteristic peaks.

XPS is an efficient equipment to analyze the elemental composition and type of chemical bonds in PN-lignin@HKUST-1. As shown in Fig. 4a, b, the P element exists in the XPS spectrum of PN-lignin@HKUST-1. Two main peaks obviously appear in the Cu2p spectrum (Fig. 4c) at 932.89 and 952.59 eV, which are attributed to Cu2p$_{3/2}$ and Cu2p$_{1/2}$, respectively. Furthermore, the spectrum shows two weak peaks at 934.31 and 954.31 eV, corresponding to the satellite peak of Cu2p$_{3/2}$ and Cu2p$_{1/2}$, respectively. In addition, the O1s spectrum of PN-lignin@HKUST-1 (Fig. 4d) is divided into three peaks appearing at 532.06, 532.98 and 533.76 eV, which are ascribed to Cu–O, C=O and C–OH, respectively [44]. The above evidences fully prove the successful preparation of flame retardant PN-lignin@HKUST-1.

Thermal behavior of prepared flame retardants

To investigate the mass-loss behavior and thermal decomposition process of lignin and flame retardants under nitrogen atmosphere, the TGA and DTG curves are presented in Fig. 5 with the detailed data listed in Table 2. The degradation route is traced by detecting the initial degradation temperature (T_i, where a mass loss of 5 mass% takes place), the maximum temperature (T_{max}, where the mass-loss rate reaches a maximum) and the mass of residue left. As can be seen from Table 2, the thermal decomposition of Al-lignin starts from 105.54 °C and shows a sharp decrease at 333.36 °C, with 41.57 mass% residue left at 800 °C. The T_i of PN-lignin and PN-lignin@HKUST-1 are both lower than that of Al-lignin. The onset degradation temperature decreases due to the incorporation of DOPO, which has a high gas-phase activity and condensed-phase activity (through char formation) [25, 45]. In addition, the O=P–O bond in DOPO is less stable than the common C–C bond, which is also responsible for the advanced decomposition. Compared with original Al-lignin, the char residues of PN-lignin and PN-lignin@HKUST-1 are reduced because of the relatively low lignin content (Fig. 5a), which are 18.24 mass% and 31.13 mass%, respectively. However, the char residue of PN-lignin@HKUST-1 is much higher than that of PN-lignin. The underlying reason is the catalytic ability of metal copper ions in HKUST-1 on the char formation process, which can contribute to protecting the
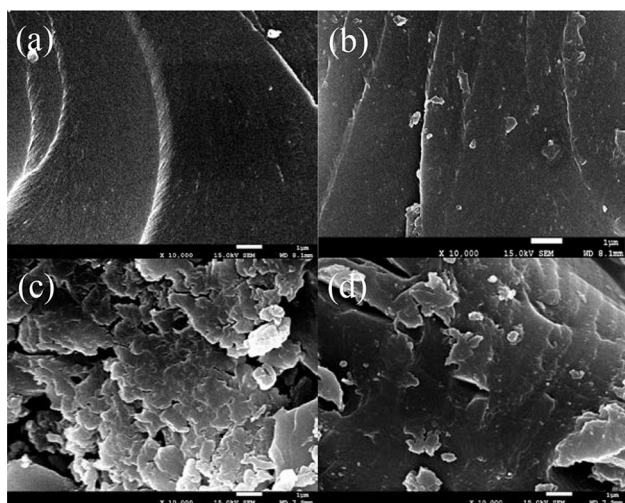
Fig. 4 XPS of spectrum of PN-lignin@HKUST-1

Fig. 5 TGA (**a**) and DTG (**b**) curves of Al-lignin, PN-lignin and PN-lignin@HKUST-1

polymer when their composites are exposed to the fire [46]. As shown in Fig. 5b, the decomposition of PN-lignin exhibits one rapid and violent degradation stage with T_{max} at about 354.73 °C, which is primarily attributed to the degradation of DOPO and MEL, along with the formation of polyphosphate and release of ammonia (NH_3), nitrogen (N_2) and water vapor (H_2O) [47, 48]. The followed stage after 450 °C is potentially assigned to the degradation of polyphosphate for the generation of phosphoric acids and metaphosphoric acids [47]. The degradation process of PN-lignin@HKUST-1 is more complicated, and the T_{max} (309.22 °C) is much lower than that of PN-lignin, on account of the introduction of foam HKUST-1, which

Table 2 TGA data of Al-lignin, PN-lignin and PN-lignin@HKUST-1 under N_2 atmosphere

Sample	T_i/°C	T_{max}/°C	Residue/mass%
Al-lignin	105.54	333.36	41.57
PN-lignin	87.10	354.73	18.24
PN-lignin@ HKUST-1	83.57	309.22	31.13

has a relatively weaker thermal stability and decomposes gradually at about 320 °C [36].

Fig. 6 SEM images of EP thermoset (**a**, **b**) and EP/PN-lignin@ HKUST-1 composite (**c**, **d**) at 10,000 times magnification
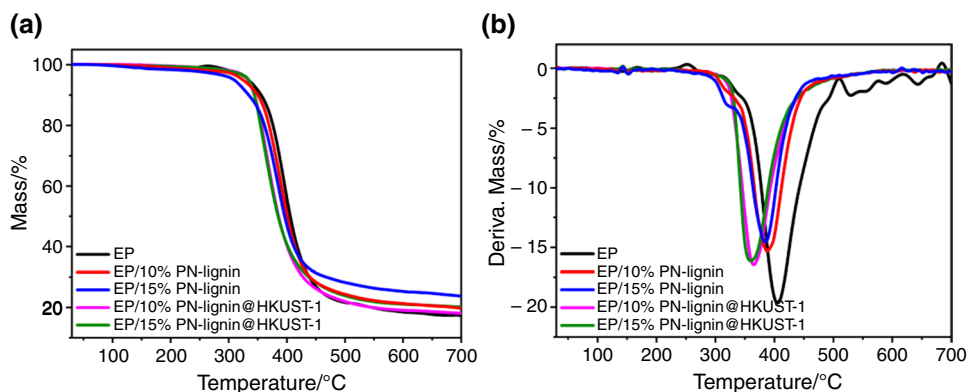
Dispersibility of flame retardant in prepared EP composites

To verify the compatibility and interfacial interaction between flame retardant and polymeric matrix, the SEM images of fractured sections for EP thermoset and EP/PN-lignin@HKUST-1 are shown in Fig. 6. It can be clearly seen that there are few folds distributed on the flat and smooth fractured surface of neat EP thermoset. Almost no embedded particles are visible under this circumstance. By contrast, a series of irregular folds and particles of different sizes on the fractured surface of EP/PN-lignin@HKUST-1 composite can be observed. This obvious difference is attributed to the inclusion of PN-lignin@HKUST-1, which implies the strong interfacial interaction between additives with EP thermoset matrix. The result shows that PN-lignin@HKUST-1 has been absolutely mixed with EP thermoset and possessed a great dispersibility in the composite.

Thermal behavior of prepared EP composites

The TGA, DTG curves of EP thermoset and its composites under N_2 atmosphere are shown in Fig. 7, and the corresponding data are listed in Table 3. The thermal decomposition process of neat EP thermoset undergoes only one main degradation step, which starts from 333.74 °C and shows a sharp decrease at 405.35 °C, leaving a char residue of 17.21 mass% at 800 °C (Fig. 7a). The T_i of EP/PN-lignin and EP/PN-lignin@HKUST-1 composites are shifted to a lower range, which can be attributed to the early degradation of the flame retardants and the catalytic effect of the metals [49]. The T_{max} of all of the additive modified composites is also brought forward to different extents compared with neat EP thermoset. It can be seen from Fig. 7b that T_{max} shows a decreasing trend as EP > EP/10% PN-lignin > EP/15% PN-lignin > EP/10% PN-lignin@HKUST-1 > EP/15% PN-lignin@HKUST-1. For intumescent flame-retardant system, the faster decomposition of flame retardants is conducive to accelerating the charring of polymeric matrix. This tendency suggests that the flame retardants can come into play at a lower temperature range, especially for EP/PN-lignin@ HKUST-1, the T_{max} of which is about 20°C lower than that of EP/PN-lignin at the same content. The early decomposition of the composite can be explained by the presence of copper irons (Cu^{2+}), which can promote the decomposition of molecular chains of polymer due to the catalytic interaction of open metal sites and unsaturated covalent bonds [49]. As shown in Table 3, the char residue of EP/PN-lignin and EP/PN-lignin@HKUST-1 is much higher than that of the EP thermoset, which increases greatly with increasing the additive amount. Therefore, the rapid degradation and catalysis of PN-lignin@HKUST-1 are beneficial for the quick formation and significant enhancement of char residue [50].

Fig. 7 TGA (**a**) and DTG (**b**) curves of EP thermoset, EP/ PN-lignin and EP/PN-lignin@ HKUST-1 composites

Flame-retardant properties of prepared EP composites

Table 4 shows the flame retardancy of EP thermoset and its composites evaluated by the limited oxygen index (LOI) and UL-94 vertical test. The LOI value of pure EP is only 26.1%, indicating that EP thermoset tends to burn easily in air. The LOI values of EP composites are improved to different degrees by the addition of flame retardants. When the amount of PN-lignin added is 10 mass%, the LOI value of EP composite is 28.5%, while has no flame-retardant rating. The LOI value increases from 28.5 to 29.8% as the amount of PN-lignin content increases from 10 to 15 mass%, and the latter just achieves V-2 rating in UL-94 vertical test. When 10 and 15 mass% of PN-lignin@HKUST-1 are applied in the EP, the LOI value remarkably increases to 31.7% and 33.2%, respectively, which suggests that it is difficult for the composites to burn under such conditions. Meanwhile, EP/10% PN-lignin@HKUST-1 can reach V-1 rating and EP/15% PN-lignin@HKUST-1 can even reach V-0 rating in UL-94 vertical test, revealing an important role of PN-lignin@HKUST-1 in restraining the inflammation. These results show that the lignin-based flame retardant modified by nitrogen and phosphorus can improve the flame-retardant properties of EP thermoset, but they may not meet the application requirements in practice. However, the LOI value and UL-94 flame retardant level of the composites can be dramatically improved when the HKUST-1 structure is introduced, which is mainly attributed to the synergistic flame-retardant effect of DOPO and HKUST-1.

Cone calorimetry test is a comprehensive evaluation method for the fire risk of polymers by monitoring many important real-time and statistical parameters throughout combustion process. The heat release rate (HRR) and total heat release (THR) curves for EP thermoset, EP/15% PN-lignin and EP/15% PN-lignin@HKUST-1 composites are given in Fig. 8, and the key combustion parameters collected from the test are listed in Table 5. The ignition time (time to ignition, TTI) of EP/15% PN-lignin and EP/15% PN-lignin@HKUST-1 composites is shorter than that of neat EP thermoset, indicating that addition of PN-lignin and PN-lignin@HKUST-1 can reduce the initial pyrolysis temperature, which is in exact accordance with the TGA results. For catalytic char formation system, the short ignition time means that flame retardants can take effect in the early combustion process, decomposing inorganic acids and metal ions to promote the formation of residue char [51, 52]. The high peak heat release rate (PHRR) and THR values of the EP thermoset are as high as 1089.6 kW m^{-2} and 155.2 MJ m^{-2}, respectively. The PHRR value is decreased to 906.5 kW m^{-2}, and the THR value is also decreased to 129.4 MJ m^{-2} as 15 mass% PN-lignin is added in the composite, which exhibits relatively good flame retardancy. While the incorporation of 15 mass% PN-lignin@HKUST-1 is capable of further reducing the values of PHRR and THR to 640.1 kW m^{-2} and 102.7 MJ m^{-2}, respectively, corresponding to 41.2 and 33.8% reductions compared to neat EP thermoset. On the one hand, PN-lignin@HKUST-1 can generate non-flammable gases such as ammonia, carbon monoxide and water vapor during combustion, which reduce the concentration of flammable gases in the polymer and absorb large amounts of heat to reduce the surface temperature [48]. On the other hand, the char residue of EP/15% PN-lignin@HKUST-1 (11.80 mass%) is far more than that of EP thermoset (0.50 mass%) and EP/15% PN-lignin (5.10 mass%). As mentioned, it mainly owes to the catalytical char formation capacity of copper ions in HKUST-1, which can facilitate the generation of protective char layer, thereby blocking the oxygen and thermal, and inhibiting the volatilization of flammable gas. Based on these results, it can be inferred that EP/PN-lignin@HKUST-1 presents the extremely superior flame retardancy.

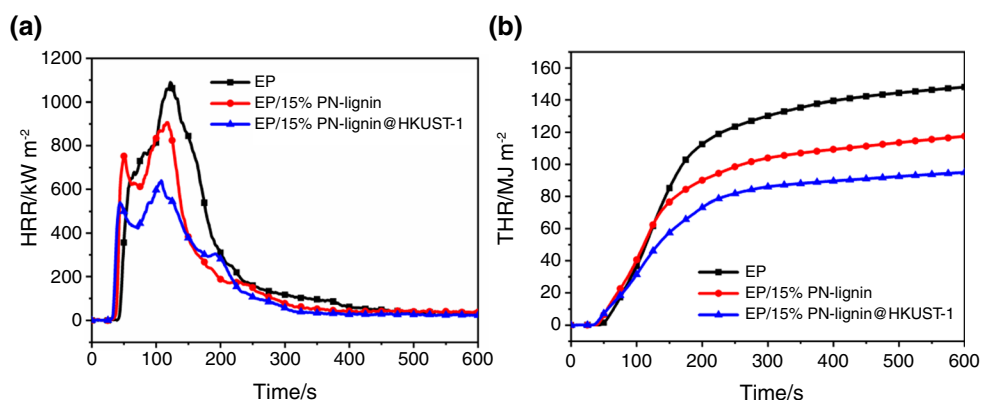**Table 3** TGA data of EP thermoset, EP/PN-lignin and EP/PN-lignin@HKUST-1 composites under N$_2$ atmosphere

Sample	T_i/°C	T_{max}/°C	Residues/mass%
EP	333.74	405.35	17.21
EP/10% PN-lignin	324.11	387.83	19.74
EP/15% PN-lignin	309.26	384.97	23.72
EP/10% PN-lignin@HKUST-1	332.62	364.96	18.05
EP/15% PN-lignin@HKUST-1	330.14	360.73	20.14

Table 4 LOI values and UL-94 vertical test results of EP thermoset, EP/PN-lignin and EP/PN-lignin@HKUST-1 composites

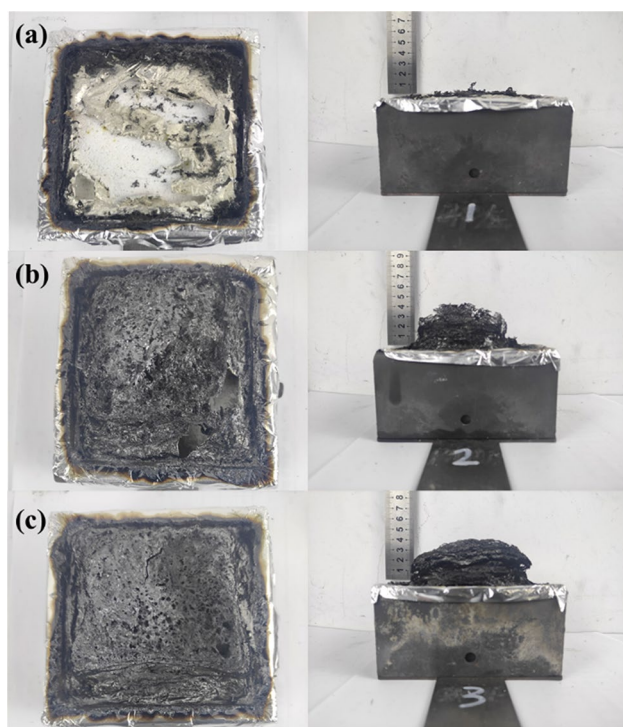| Sample	EP/mass%	DDM/mass%	PN-lignin/mass%	PN-lignin@HKUST-1/mass%	LOI/%	UL-94 rating
EP	83.3	16.7	–	–	26.1	V-2
EP/10% PN-lignin	75.0	15.0	10.0	–	28.5	V-2
EP/15% PN-lignin	70.8	14.2	15.0	–	29.8	V-2
EP/10% PN-lignin@HKUST-1	75.0	15.0	–	10.0	31.7	V-1
EP/15% PN-lignin@HKUST-1	70.8	14.2	–	15.0	33.2	V-0

Fig. 8 HRR (**a**) and THR (**b**) curves of EP thermoset, EP/15% PN-lignin and EP/15% PN-lignin@HKUST-1 composites
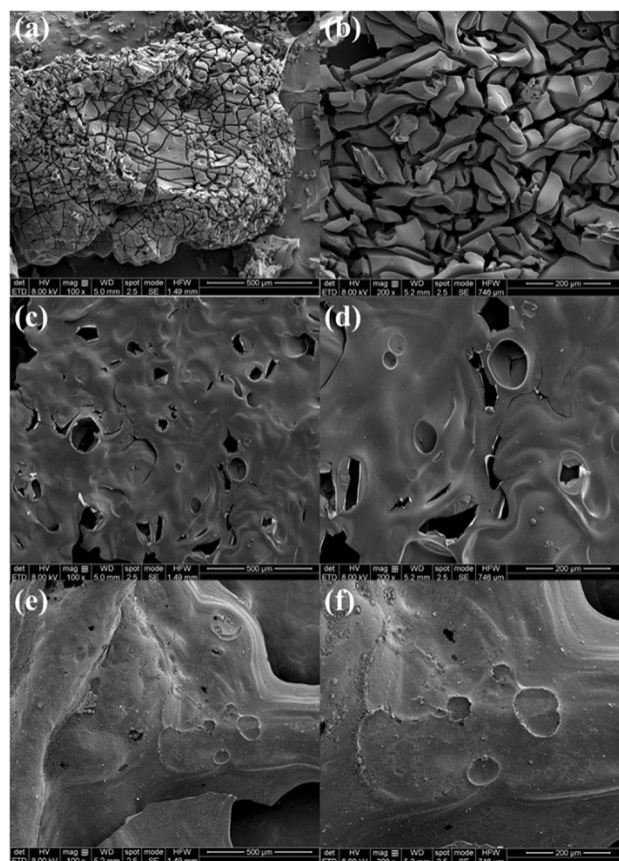

Table 5 Detailed data obtained from cone calorimeter tests of EP thermoset, EP/15% PN-lignin and EP/15% PN-lignin@HKUST-1 composites

Sample	EP	EP/15% PN-lignin	EP/15% PN-lignin@HKUST-1
TTI (s)	45	37	33
THR/MJ m^{-2}	155.2	129.4	102.7
PHRR/kW m^{-2}	1089.6	906.5	640.1
av-EHC/MJ kg^{-1}	28.06	34.40	20.98
TSP/m^2	34.8	35.7	37.9
av-COY/kg kg^{-1}	0.439	0.601	0.237
av-CO_2Y/kg kg^{-1}	2.821	3.394	2.016
Residue/mass%	0.50	5.10	11.80

Apart from the heat release, the release of smoke and toxic gases is another factor to consider for flame-retardant additives, especially carbon monoxide, which constitutes a fatal disadvantage of traditional phosphorous-containing flame retardants in practical applications [49]. Compared with the smoke release of the neat EP thermoset, the incorporation of PN-lignin and PN-lignin@HKUST-1 mildly increases the total smoke production (TSP) of composite materials. However, the average carbon monoxide yield
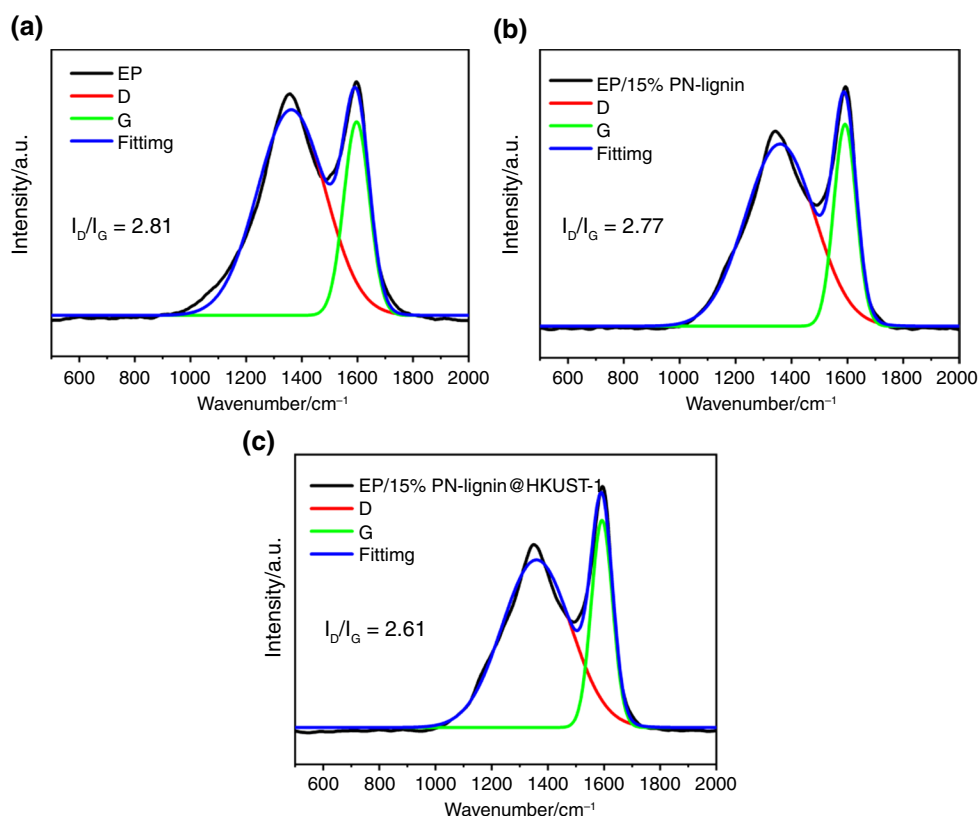

Fig. 9 Digital photographs of char residues of EP thermoset (**a**), EP/15% PN-lignin (**b**) and EP/15% PN-lignin@HKUST-1 (**c**) composites after cone calorimeter test

Fig. 10 SEM images of chars for EP thermoset (**a**, **b**), EP/15% PN-lignin (**c**, **d**) and EP/15% PN-lignin@HKUST-1 (**e**, **f**) composites at 10,000 times magnification

Fig. 11 LRS spectra of the residues of EP thermoset (**a**), EP/15% PN-lignin (**b**), EP/15% PN-lignin@HKUST-1 (**c**) composites

(av-COY) of EP/15% PN-lignin@HKUST-1 composite is 0.237 kg kg^{-1}, about half that– of the EP thermoset (0.439 kg kg^{-1}). It is mainly attributed to HKUST-1, which can provide active catalytic centers for the oxidation of CO [53]. Moreover, HKUST-1 also can absorb gases released because of its high porosity and large specific surface area. Therefore, the average carbon dioxide yield (av-CO$_2$Y) of EP/15% PN-lignin@HKUST-1 composite (2.016 kg kg^{-1}) is much lower than that of the EP thermoset (2.821 kg kg^{-1}) [54, 55]. It is reasonable to conclude that PN-lignin@HKUST-1 possesses outstanding flame-retardant ability, for the reason that it can reduce the exothermic rate, increase the amount of char residue, and inhibit the production of harmful gases.

Char residue analysis of prepared EP composites

Figure 9 shows the digital photographs of EP thermoset, EP/15% PN-lignin and EP/15% PN-lignin@HKUST-1 composites after cone calorimetry test. The neat EP sample is almost burnt out with nearly no char residue left, while the other two composites have much more char yields in favor of serving as a isolated layer. It can be seen that a certain degree of swelling occurs after the combustion of EP/15% PN-lignin, but the surface of char layer appears to be loose and irregular, which cannot prevent the material

well from burning. In comparison, the addition of 15 mass% PN-lignin@HKUST-1 can form a dense char layer on the surface, accompanied with a regular appearance and significant expansion. It is due to the combined effects of DOPO and HKUST-1: the polyacids, metal ions and metal oxides generated by decomposition at high temperatures catalyze the formation and dehydration of char layer, resulting in a more compact and intact structure. Furthermore, the non-flammable gas produced by thermal decomposition greatly expands the char layer, thus isolating the oxygen and achieving the purpose of flame retardant.

As shown in Fig. 10, SEM images are investigated to further measure the morphology of char residue of EP thermoset and its composites after the cone calorimetry test. The char layer of neat EP is cracked and fractured, whereas EP/15% PN-lignin tends to form an unbroken and compact char layer that can act as a shield against the transfer of gases and heat. However, many broken pores can still be clearly observed on the surface, which is probably due to the gases flushing out from the weak points of char layer. By contrast, the pores on the char layer of EP/15% PN-lignin@HKUST-1 nearly disappeared after the introduction of HKUST-1, as evidenced by the high char residue and gas absorption capacity. Such a dense and complete protective layer cannot only isolate the oxygen and heat, but also effectively prevents the escape of toxic gases and smoke [56]. The

conclusions obtained by the SEM images are in agreement with the digital graphs shown above.

Figure 11 shows the Raman spectra of the char layer of EP thermoset, EP/15% PN-lignin and EP/15% PN-lignin@ HKUST-1 composites. There are two strong absorption peaks in the Raman spectra of the three samples, near 1356 and 1593 cm^{-1}, respectively, which are the representative peaks of graphite (G and D peaks). Generally speaking, the ratio of the integrated intensities of D to G band (I_D/I_G) is usually used to assess the degree of char layer. The lower ratio of I_D/I_G means the higher graphitization degree of carbon layer, indicating that the layer is denser [57]. The I_D/I_G value of the neat EP thermoset and EP/15% PN-lignin is 2.81 and 2.77, respectively, indicating that the graphitization degree of char layer is very low. However, the I_D/I_G value of the EP composite is further decreased to 2.61 after adding PN-lignin@HKUST-1. The metal irons in the HKUST-1 can act as catalysts to generate more graphitized carbon during combustion, which contributes to the formation of char structure with improved thermal stability.

Conclusions

In this work, flame retardant PN-lignin@HKUST-1 is developed through the dual modification of phenolated Al-lignin by MEL-DOPO and HKUST-1. The acquired PN-lignin@ HKUST-1 is further added into epoxy resin (EP) to prepared flame-retardant (EP/PN-lignin@HKUST-1) composites using physical blending method. The FTIR, XRD and XPS spectra demonstrate that DOPO and HKUST-1 are successfully introduced into modified lignin. The SEM morphological observation proves that PN-lignin@ HKUST-1 in EP composite possesses great compatibility and dispersibility. Compared with PN-lignin, PN-lignin@ HKUST-1 displays excellent flame-retardant properties and pretty good catalytical char formation capacity in the EP composites. It is concluded that EP/15% PN-lignin@ HKUST-1 can reach up to V-0 rating in UL-94 vertical test and the limited oxygen index (LOI) value is 33.2%. The peak heat release rate (PHRR) and total heat release (THR) of EP composite with 15 mass% PN-lignin@HKUST-1 are 640.1 kW m^{-2} and 102.7 MJ m^{-2}, respectively. The average carbon monoxide yield (av-COY) of EP/15% PN-lignin@ HKUST-1 is 0.237 kg kg^{-1} and the average carbon dioxide yield (av-CO_2Y) is (2.016 kg kg^{-1}). These results indicate that PN-lignin@HKUST-1 can reduce the exothermic rate, increase the amount of char residue and inhibit the production of harmful gases. In addition, EP/15% PN-lignin@ HKUST-1 forms a dense and compact char layer, which can block the internal material from exposure to heat and oxygen in combustion process.

Declarations

References

1. Auvergne R, Caillol S, David G, Boutevin B, Pascault JP. Biobased thermosetting epoxy: present and future. Chem Rev. 2014;114(2):1082–115. https://doi.org/10.1021/cr3001274.

2. Gu H, Ma C, Gu J, Guo J, Yan X, Huang J, Zhang Q, Guo Z. An overview of multifunctional epoxy nanocomposites. J Mater Chem C. 2016;4:5890–906. https://doi.org/10.1039/C6TC01210H.

3. Jian XY, He Y, Li YD, Wang M, Zeng JB. Curing of epoxidized soybean oil with crystalline oligomeric poly(butylene succinate) towards high performance and sustainable epoxy resins. Chem Eng J. 2017;326:875–85. https://doi.org/10.1016/j.cej.2017.06.039.

4. Wan JT, Bu ZY, Xu CJ, Li BG, Fan H. Preparation, curing kinetics, and properties of a novel low-volatile starlike aliphatic-polyamine curing agent for epoxy resins. Chem Eng J. 2011;171(1):357–67. https://doi.org/10.1016/j.cej.2011.04.004.

5. Raquez JM, Deléglise M, Lacrampe MF, Krawczak P. Thermosetting (bio) materials derived from renewable resources: a critical review. Prog Polym Sci. 2010;35(4):487–509. https://doi.org/10.1016/j.progpolymsci.2010.01.001.

6. Chen ZK, Yang G, Yang JP, Fu SY, Ye L, Huang YG. Simultaneously increasing cryogenic strength, ductility and impact resistance of epoxy resins modified by *n*-butyl glycidyl ether. Polymer. 2009;50(5):1316–23. https://doi.org/10.1016/j.polymer.2008.12.048.

7. Wang X, Song L, Xing WY, Lu HD, Hu Y. A effective flame retardant for epoxy resins based on poly(DOPO substituted dihydroxyl phenyl pentaerythritol diphosphonate). Mater Chem Phys. 2011;125(3):536–41. https://doi.org/10.1016/j.matchemphys.2010.10.020.

8. Zhang JH, Mi XQ, Chen SY, Xu ZJ, Zhang DH, Miao MH, Wang JS. A bio-based hyperbranched flame retardant for epoxy resins. Chem Eng J. 2020;381:122719. https://doi.org/10.1016/j.cej.2019.122719.

9. Levchik SV, Weil ED. A review of recent progress in phosphorus-based flame retardants. J Fire Sci. 2006;24(5):345–64. https://doi.org/10.1177/0734904106068426.

10. Song PA, Cao ZH, Fu SY, Fang ZP, Wu Q, Ye JW. Thermal degradation and flame retardancy properties of ABS/lignin: Effects of lignin content and reactive compatibilization. Polym Degrad Stab. 2016;518(1–2):59–65. https://doi.org/10.1016/j.tca.2011.02.007.

11. Cao L, Iris KM, Liu Y, Ruan X, Tsang DC, Hunt AJ, Zhang S. Lignin valorization for the production of renewable chemicals: state-of-the-art review and future prospects. Bioresour Technol. 2018;269:465–75. https://doi.org/10.1016/j.biortech.2018.08.065.

12. Hu J, Xiao R, Shen DK, Zhang HY. Structural analysis of lignin residue from black liquor and its thermal performance in thermogravimetric-Fourier transform infrared spectroscopy. Bioresour Technol. 2013;128:633–9. https://doi.org/10.1016/j.biortech.2012.10.148.

13. Kumar A, Kumar A, Kumar J, Bhaskar T. Catalytic pyrolysis of soda lignin over zeolites using pyrolysis gas chromatography-mass spectrometry. Bioresour Technol. 2019;291:121822. https://doi.org/10.1016/j.biortech.2019.121822.

14. Pandey MP, Kim CS. Lignin depolymerization and conversion: a review of thermochemical methods. Chem Eng Technol. 2011;34(1):29–41. https://doi.org/10.1002/ceat.201000270.

15. Li B, Zhang XC, Su RZ. An investigation of thermal degradation and charring of larch lignin in the condensed phase: the effects of boric acid, guanyl urea phosphate, ammonium dihydrogen phosphate and ammonium polyphosphate. Polym Degrad Stab. 2002;75(1):35–44. https://doi.org/10.1016/S0141-3910(01)00202-6.

16. Ferry L, Dorez G, Taguet A, Otazaghine B, Lopez-Cuesta JM. Chemical modification of lignin by phosphorus molecules to improve the fire behavior of polybutylene succinate. Polym Degrad Stab. 2015;113:135–43. https://doi.org/10.1016/j.polymdegradstab.2014.12.015.

17. Yu YM, Fu SY, Song PA, Luo XP, Jin YM, Lu FZ, Wu Q, Ye JW. Functionalized lignin by grafting phosphorusnitrogen improves the thermal stability and flame retardancy of polypropylene. Polym Degrad Stab. 2012;97(4):541–6. https://doi.org/10.1016/j.polymdegradstab.2012.01.020.

18. Sandra GF, Martin G, Bernhard S, Corcuera MA, Arantxa E. Impact of the combined use of layered double hydroxides, lignin and phosphorous polyol on the fire behavior of flexible polyurethane foams. Ind Crop Prod. 2018;125:346–59. https://doi.org/10.1016/j.indcrop.2018.09.018.

19. Wu W, He HB, Liu T, Wei RC, Cao XW, Sun QJ, Venkatesh S, Yuen RKK, Roy VAL, Li RKY. Synergetic enhancement on flame retardancy by melamine phosphate modified lignin in rice husk ash filled P34HB biocomposites. Compos Sci Technol. 2018;168:246–54. https://doi.org/10.1016/j.compscitech.2018.09.024.

20. Lu X, Guo H, Que H, Wang D, Liang D, He T, Robin HM, Xu C, Zhang X, Gu X. Pyrolysis mechanism and kinetics of high-performance modified lignin-based epoxy resins. J Anal Appl Pyrolysis. 2021;154: 105013. https://doi.org/10.1016/j.jaap.2020.105013.

21. Jian RK, Ai YF, Xia L, Zhao LJ, Zhao HB. Single component phosphamide-based intumescent flame retardant with potential reactivity towards low flammability and smoke epoxy resins. J Hazard Mater. 2019;371:529–39. https://doi.org/10.1016/j.jhazmat.2019.03.045.

22. Khanal S, Zhang W, Ahmed S, Ali M, Xu S. Effects of intumescent flame retardant system consisting of tris (2-hydroxyethyl) isocyanurate and ammonium polyphosphate on the flame retardant properties of high-density polyethylene composites. Compos A Appl Sci Manufac. 2018;112:444–51. https://doi.org/10.1016/j.compositesa.2018.06.030.

23. Feng YZ, Li XW, Zhao XY, Ye YS, Zhou XP, Liu H, Liu CT, Xie XL. Synergetic improvement in thermal conductivity and flame retardancy of epoxy/silver nanowires composites by incorporating "branch-like" flame-retardant functionalized grapheme. ACS Appl Mater Inter. 2018;10(25):21628–41. https://doi.org/10.1021/acsami.8b05221.

24. Qiu Y, Qian LJ, Feng HS, Jin SL, Hao JW. Toughening effect and flame-retardant behaviors of phosphaphenanthrene/phenyl-siloxane bigroup macromolecules in epoxy thermoset. Macromolecules. 2018;51(23):9992–10002. https://doi.org/10.1021/acs.macromol.8b02090.

25. Zhang Y, Yu B, Wang BB, Liew KM, Song L, Wang CM, Hu Y. Highly effective P-P synergy of a novel DOPO-based flame retardant for epoxy resin. Ind Eng Chem Res. 2017;56(5):1245–55. https://doi.org/10.1021/acs.iecr.6b04292.

26. Jian RK, Wang P, Duan WS, Wang JS, Zheng XL, Weng JB. Synthesis of a novel P/N/S- containing flame retardant and its application in epoxy resin: thermal property, flame retardance, and pyrolysis behavior. Ind Eng Chem Res. 2016;55:11520–7. https://doi.org/10.1021/acs.iecr.6b03416.

27. Wang J, Ma C, Wang P, Qiu S, Cai W, Hu Y. Ultra-low phosphorus loading to achieve the superior flame retardancy of epoxy resin. Polym Degrad Stab. 2018;149:119–28. https://doi.org/10.1016/j.polymdegradstab.2018.01.024.

28. Lu X, Zhu X, Dai P, Robin HM, Guo H, Que H, Wang D, Liang D, He T, Xu C, Luo Z, Gu X. Thermal performance and thermal decomposition kinetics of a novel lignin-based epoxy resin containing phosphorus and nitrogen elements. J Therm Anal Calorim. 2022;147:5237–53. https://doi.org/10.1007/s10973-021-10950-9.

29. Zhang Y, Zhang S, Chung TS. Nanometric graphene oxide framework membranes with enhanced heavy metal removal via nanofiltration. Environ Sci Technol. 2015;49(16):10235–42. https://doi.org/10.1021/acs.est.5b02086.

30. Han Y, Jiang Y, Gao C. High-flux graphene oxide nanofiltration membrane intercalated by carbon nanotubes. ACS Appl Mater Inter. 2015;7(15):8147–55. https://doi.org/10.1021/acsami.5b00986.

31. Janakiram S, Espejo JLM, Yu X, Ansaloni L, Deng L. Facilitated transport membranes containing graphene oxide-based nanoplatelets for CO_2 separation: effect of 2D filler properties. J Membrane Sci. 2020;616:118626. https://doi.org/10.1016/j.memsci.2020.118626.

32. Li ZQ, Li CX, Ge XL, Ma JY, Zhang ZW, Li Q, Wang CX, Yin LW. Reduced graphene oxide wrapped MOFs-derived cobalt-doped porous carbon polyhedrons as sulfur immobilizers as cathodes for high performance lithium sulfur batteries. Nano Energy. 2016;23:15–26. https://doi.org/10.1016/j.nanoen.2016.02.049.

33. Chae HK, Siberio-Pérez DY, Kim J, Go Y, Eddaoudi M, Matzger AJ, O'Keeffe M, Yaghi OM. A route to high surface area porosity and inclusion of large molecules in crystals. Nature. 2004;427:523–7. https://doi.org/10.1038/nature02311.

34. Rieter WJ, Taylor KML, An H, Lin W, Lin W. Nanoscale metal-organic frameworks as potential multimodal contrast enhancing agents. J Am Chem Soc. 2006;128(28):9024–5. https://doi.org/10.1021/ja0627444.

35. Kesanli B, Lin W. Chiral porous coordination networks: rational design and applications in enantioselective processes. Coord Chem Rev. 2003;246(1–2):305–26. https://doi.org/10.1016/j.cct.2003.08.004.

36. Cui XF, Sun XD, Liu L, Huang QH, Yang HC, Chen CJ, Nie SX, Zhao ZX, Zhao ZX. In-situ fabrication of cellulose foam HKUST-1 and surface modification with polysaccharides for enhanced selective adsorption of toluene and acidic dipeptides. Chem Eng J. 2019;369:898–907. https://doi.org/10.1016/j.cej.2019.03.129.

37. Liu LN, Qian MB, Song PA, Huang GB, Yu YM, Fu SY. Fabrication of green lignin-based flame retardants for enhancing the thermal and fire retardancy properties of polypropylene/wood composites. ACS Sustain Chem Eng. 2016;4(4):2422–31. https://doi.org/10.1021/acssuschemeng.6b00112.

38. Back S, Lim J, Kim N, Kim Y, Jung Y. Single-atom catalysts for CO_2 electroreduction with significant activity and selectivity improvements. Chem Sci. 2017;8:1090–6. https://doi.org/10.1039/C6SC03911A.

39. Gaan S, Liang S, Mispreuve H, Perler H, Naescher R, Neisius M. Flame retardant flexible polyurethane foams from novel DOPO-phosphonamidate additives. Polym Degrad Stab. 2015;113:180–8. https://doi.org/10.1016/j.polymdegradstab.2015.01.007.

40. Wang X, Hu Y, Song L, Xing W, Lu H, Lv P, Jie G. Flame retardancy and thermal degradation mechanism of epoxy resin composites based on a DOPO substituted organophosphorus oligomer. Polymer. 2010;51(11):2435–45. https://doi.org/10.1016/j.polymer.2010.03.053.

41. Wang B, Yang X, Qiao C, Li Y, Li T, Xu C. Effects of chitosan quaternary ammonium salt on the physicochemical properties of sodium carboxymethyl cellulosebased films. Carbohyd Polym. 2018;184:37–46. https://doi.org/10.1016/j.carbpol.2017.12.030.

42. Liu Q, Jin L, Sun W. Facile fabrication and adsorption property of a nano/microporous coordination polymer with controllable size and morphology. Chem Commun. 2012;48(70):8814–6. https://doi.org/10.1039/C2CC34192A.

43. Dai XQ, Hang YH, Zhao X, Sun C, Ju LN, Gui XJ, Sun S, Xu YB, Wang YR, Li YF. ZIF-8 as an adsorbent of aqueous phase for Eu and Tb ions. Micro Nano Lett. 2017;12(3):187–90. https://doi.org/10.1049/mnl.2016.0674.

44. Dong L, Jiao F, Qin W, Zhu H, Jia W. New insights into the carboxymethyl cellulose adsorption on scheelite and calcite: adsorption mechanism, AFM imaging and adsorption model. Appl Surf Sci. 2019;463:105–14. https://doi.org/10.1016/j.apsusc.2018.08.192.

45. Perret B, Schartel B, Stöß K, Ciesielski M, Diederichs J, Döring M, Krämer J, Altstädt V. Novel DOPO-based flame retardants in high-performance carbon fiber epoxy composites for aviation. Eur Polym J. 2011;47(5):1081–9. https://doi.org/10.1016/j.eurpolymj.2011.02.008.

46. Liu LN, Huang GB, Song PA, Yu YM, Fu SY. Converting industrial alkali lignin to biobased functional additives for improving fire behavior and smoke suppression of polybutylene succinate. ACS Sustain Chem Eng. 2016;4(9):4732–42. https://doi.org/10.1021/acssuschemeng.6b00955.

47. Jin X, Sun J, Zhang JS, Gu X, Bourbigot S, Li H, Tang W, Zhang S. Preparation of a novel intumescent flame retardant based on supramolecular interactions and its application in polyamide 11. ACS Appl Mater Inter. 2017;9(29):24964–75. https://doi.org/10.1021/acsami.7b06250.

48. Lu X, Yu M, Wang D, Xiu P, Xu C, Lee AF, Gu X. Flame-retardant effect of a functional DOPO-based compound on lignin-based epoxy resins. Mater Today Chem. 2021;22:100562. https://doi.org/10.1016/j.mtchem.2021.100562.

49. Qi XL, Zhou DD, Zhang J, Hu S, Haranczyk M, Wang DY. Simultaneous improvement of mechanical and fire-safety properties of polymer composites with phosphonate-loaded MOF additives. ACS Appl Mater Inter. 2019;11:20325–32. https://doi.org/10.1021/acsami.9b02357.

50. Liao SH, Liu PL, Hsiao MC, Teng CC, Wang CA, Ger MD, Chiang CL. One-step reduction and functionalization of graphene oxide with phosphorus-based compound to produce flame-retardant epoxy nanocomposite. Ind Eng Chem Res. 2012;51:4573–81. https://doi.org/10.1021/ie2026647.

51. Tang S, Qian LJ, Liu XX, Dong YP. Gas-phase flame-retardant effects of a bi-group compound based on phosphaphenanthrene and triazine-trione groups in epoxy resin. Polym Degrad Stab. 2016;133:350–7. https://doi.org/10.1016/j.polymdegradstab.2016.09.014.

52. Ma C, Yu B, Hong NN, Pan Y, Hu WZ, Hu Y. Facile synthesis of a highly efficient, halogen-free, and intumescent flame retardant for epoxy resins: thermal properties, combustion behaviors, and flame-retardant mechanisms. Ind Eng Chem Res. 2016;55:10868–79. https://doi.org/10.1021/acs.iecr.6b01899.

53. Alaerts L, Seguin E, Poelman H, Thibault-Starzyk F, Jacobs P, De Vos DE. Probing the lewis acidity and catalytic activity of the metal-organic framework $[Cu_3(btc)_2]$ (BTC=benzene-1,3,5-tricarboxylate). Chem Eur J. 2006;12(28):7353–63. https://doi.org/10.1002/chem.200600220.

54. Li X, Yang X, Xue H, Pang H, Xu Q. Metal–organic frameworks as a platform for clean energy applications. J Energy Chem. 2020;2(2):100027. https://doi.org/10.1016/j.enchem.2020.100027.

55. Ryu U, Jee S, Rao PC, Shin J, Ko C, Yoon M, Park KS, Choi KM. Recent advances in process engineering and upcoming applications of metal–organic frameworks. Coord Chem Rev. 2021;426:213544. https://doi.org/10.1016/j.ccr.2020.213544.

56. Lu X, Gu X. Fabrication of a bi-hydroxyl-bi-DOPO compound with excellent quenching and charring capacities for lignin-based epoxy resin. Int J Biol Macromol. 2022;205:539–52. https://doi.org/10.1016/j.ijbiomac.2022.02.103.

57. Xu WZ, Zhang BL, Wang XL, Wang GS, Ding D. The flame retardancy and smoke suppression effect of a hybrid containing $CuMoO_4$ modified reduced graphene oxide/layered double hydroxide on epoxy resin. J Hazard Mater. 2018;343:364–75. https://doi.org/10.1016/j.jhazmat.2017.09.057.

Authors and Affiliations

Hongyu Yang[1] · Yu Qin[1] · Dingxiang Liang[1] · Xinyu Lu[1] · Xiaoli Gu[1]

✉ Xinyu Lu
NJFULXY@outlook.com

✉ Xiaoli Gu
guxiaoli@njfu.edu.cn

1   Jiangsu Co-Innovation Center of Efficient Processing and Utilization of Forest Resources, College of Chemical Engineering, Nanjing Forestry University, Nanjing 210037, China